ウエスタンブロット解析

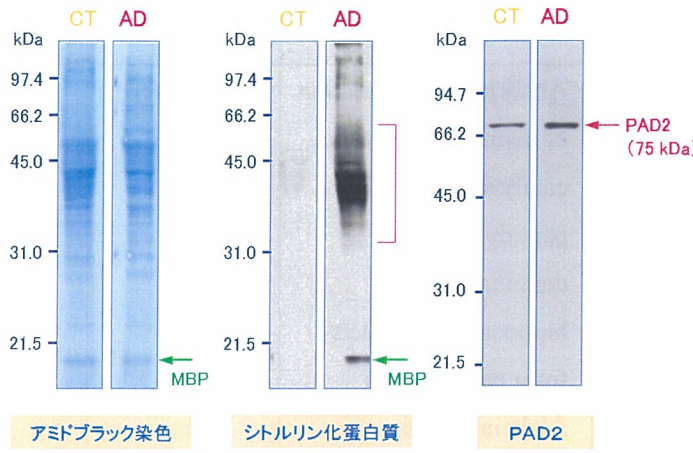

MBP (18 kDa):ミエリン塩基性蛋白質

★ AD脳ではシトルリン化蛋白質、
PAD2が多く存在する。

図　1

プロテオーム解析による シトルリン化蛋白質の同定

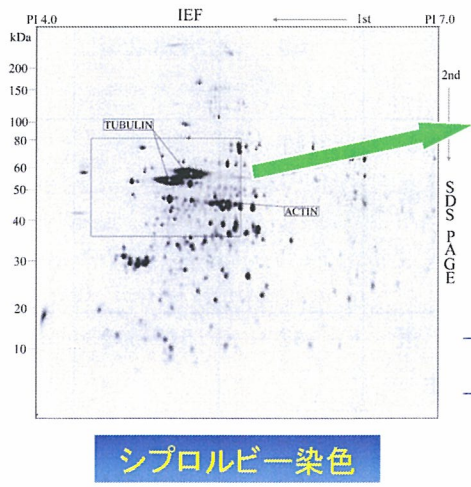

シプロルビー染色

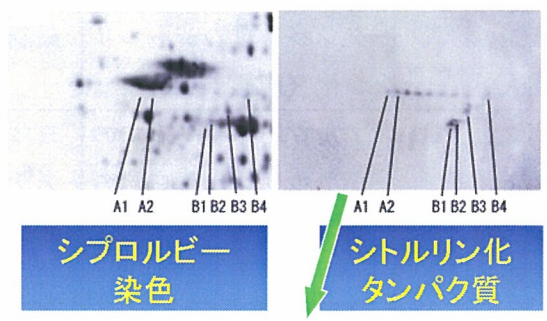

シプロルビー染色　　シトルリン化タンパク質

スポット番号	シトルリン化タンパク質
A1, A2	ビメンチン
B1, B2, B3, B4	グリア線維性酸性タンパク質 (GFAP)

図　2

III. 研究成果の刊行に関する一覧表

雑誌

発表者氏名	論文タイトル名	発表誌名	巻号	ページ	出版年
Ishigami, A., Ohsawa, T., Hiratsuka, M., Taguchi, H., Kobayashi, S., Saito, Y., Murayama, S., Asaga, H., Toda, T., Kimura, N., Maruyama, N.	Abnormal accumulation of deiminated proteins catalyzed by peptidylarginine deiminase in hippocampal extracts from patients with Alzheimer's disease.	J. Neurosci. Res	80	120-128	2005
Feng, D., Imasawa, T., Nagano, T., Kikkawa, M., Takayanagi, K., Ohsawa, T., Akiyama, K., Ishigami, A., Toda, T., Mitarai, T., Machida, T. Maruyama, N.	Citrullination preferentially proceeds in glomerular Bowman's capsule and increases in obstructive nephropathy.	Kidney Int.	68	84-95	2005
丸山直記、石神昭人	タンパク質のシトルリン化と病態	最新医学	60	2498-2501	2005
石神昭人、山本尚吾、田口ひろみ、丸山直記	アルツハイマー病でのシトルリン化蛋白質の異常な蓄積	日本未病システム学会雑誌	11	84-85	2005
丸山直記、石神昭人	老年病におけるシトルリン化蛋白質の病態生理学的意義	日本老年医学会雑誌	42	519-522	2005
丸山直記、石神昭人、近藤嘉高	老化の分子異常～臨床検査医学への貢献	臨床病理	53	728-734	2005

Journal of Neuroscience Research 80:120–128 (2005)

Abnormal Accumulation of Citrullinated Proteins Catalyzed by Peptidylarginine Deiminase in Hippocampal Extracts From Patients With Alzheimer's Disease

Akihito Ishigami,[1]* Takako Ohsawa,[2] Masaharu Hiratsuka,[3] Hiromi Taguchi,[1] Saori Kobayashi,[1] Yuko Saito,[4] Shigeo Murayama,[4] Hiroaki Asaga,[5] Tosifusa Toda,[6] Narimichi Kimura,[2] and Naoki Maruyama[1]

[1]Department of Molecular Pathology, Tokyo Metropolitan Institute of Gerontology, Itabashi-ku, Tokyo, Japan
[2]Cellular Signaling Research Group, Tokyo Metropolitan Institute of Gerontology, Itabashi-ku, Tokyo, Japan
[3]Department of Molecular and Cell Genetics, Graduate School of Medical Science, Tottori University, Tottori-shi, Tottori, Japan
[4]Department of Neuropathology, Tokyo Metropolitan Institute of Gerontology, Itabashi-ku, Tokyo, Japan
[5]Biological Science Laboratory, Meiji University, Suginami-ku, Tokyo, Japan
[6]Proteomics Collaboration Research Group, Tokyo Metropolitan Institute of Gerontology, Itabashi-ku, Tokyo, Japan

Citrullinated proteins are the products of a posttranslational process in which arginine residues undergo modification into citrulline residues when catalyzed by peptidylarginine deiminases (PADs) in a calcium ion-dependent manner. In our previous report, PAD2 expressed mainly in the rat cerebrum became activated early in the neurodegenerative process. To elucidate the involvement of protein citrullination in human neuronal degeneration, we examined whether citrullinated proteins are produced during Alzheimer's disease (AD). By Western blot analysis with antimodified citrulline antibody, citrullinated proteins of varied molecular weights were detected in hippocampal tissues from patients with AD but not normal humans. Two of the citrullinated proteins were identified as vimentin and glial fibrillary acidic protein (GFAP) by using two-dimensional gel electrophoresis and MALDI-TOF mass spectrometry. Interestingly, PAD2 was detected in hippocampal extracts from AD and normal brains, but the amount of PAD2 in the AD tissue was markedly greater. Histochemical analysis revealed citrullinated proteins throughout the hippocampus, especially in the dentate gyrus and stratum radiatum of CA1 and CA2 areas. However, no citrullinated proteins were detected in the normal hippocampus. PAD2 immunoreactivity was also ubiquitous throughout both the AD and the normal hippocampal areas. PAD2 enrichment coincided well with citrullinated protein positivity. Double immunofluorescence staining revealed that citrullinated protein- and PAD2-positive cells also coincided with GFAP-positive cells, but not all GFAP-positive cells were positive for PAD2. As with GFAP, which is an astrocyte-specific marker protein, PAD2 is distributed mainly in astrocytes. These collective results, the abnormal accumulation of citrullinated proteins and abnormal activation of PAD2 in hippocampi of patients with AD, strongly suggest that PAD has an important role in the onset and progression of AD and that citrullinated proteins may become a useful marker for human neurodegenerative diseases. © 2005 Wiley-Liss, Inc.

Key words: Alzheimer's disease; astrocyte; citrulline; glial fibrillary acidic protein; PAD; vimentin

Numerous proteases and posttranslational modification enzymes participate in neurodegeneration, such as that in patients with Alzheimer's disease (AD) and Parkinson's disease (Keller et al., 2000; Maccioni et al., 2001). However, little attention has been paid to one such group of agents, peptidylarginine deiminases (PADs; EC 3.5.3.15; Rogers and Simmonds, 1958; Kubilus et al., 1980; Kubilus and Baden, 1983; Ishigami et al., 1996). PADs are a group of posttranslational modification enzymes that citrullinate (deiminate) protein arginine residues in a calcium ion-dependent manner, yielding citrulline residues. Enzymatic citrullination abolishes positive charges of native protein molecules, inevitably causing significant alterations in their structure and functions (Lamensa and Moscarello, 1993; Imparl et al., 1995; Tarcsa et al., 1996). In mammalian tissues, PADs are found as

*Correspondence to: Akihito Ishigami, PhD, Department of Molecular Pathology, Tokyo Metropolitan Institute of Gerontology, 35-2 Sakae-cho, Itabashi-ku, Tokyo 173-0015, Japan. E-mail: ishigami@tmig.or.jp

Received 4 October 2004; Revised 22 December 2004; Accepted 4 January 2005

Published online 9 February 2005 in Wiley InterScience (www.interscience.wiley.com). DOI: 10.1002/jnr.20431

TABLE I. Subject Demographic Data*

	Age (years)	PMI (hr)	Gender	BW (g)	Braak stage NFT	Braak stage SP
AD	84.5 ± 1.4	7.9 ± 2.1	3 M/7 F	1,104 ± 99	VI (10)	C (10)
Control	79.2 ± 1.6	6.5 ± 2.4	5 M/4 F	1,226 ± 31	I (9)	0 (6), A (3)

*Data are expressed as mean ± SEM. Parentheses indicated the number of subject. PMI, post-mortem interval; BW, brain weight; NFT, neurofibrillary tangle; SP, senile plaque; AD, Alzheimer disease.

five different isoforms (i.e, types 1–4, 6), which differ in specificity for various synthetic substrates, such as benzoyl-L-arginine ethyl ester and benzoyl-L-arginine, and in tissue distribution (Watanabe et al., 1988; Terakawa et al., 1991; Chavanas et al., 2004). All these isoforms display nearly identical amino acid sequences (Watanabe and Senshu, 1989; Tsuchida et al., 1993; Nishijyo et al., 1997; Ishigami et al., 1998; Nakashima et al., 1999; Rus'd et al., 1999), but they appear to be dissimilar in tissue-specific expression, as evidenced by reverse transcriptase-polymerase chain reaction (Ishigami et al., 2001). Among them, only PAD2 has been proved to be an occupant of the rat central nervous system (Kubilus and Baden, 1983; Watanabe et al., 1988; Terakawa et al., 1991). Immunocytochemical studies have localized PAD2 in glial cells, especially astrocytes (Vincent et al., 1992; Asaga and Ishigami, 2000, 2001), microglial cells (Vincent et al., 1992; Asaga et al., 2002), and oligodendrocytes (Akiyama et al., 1999). Because citrullinated proteins were rarely located in the enzyme-positive glial cells examined with our sensitive detection method (Senshu et al., 1992), we assumed that PAD2 is normally inactive (Asaga and Ishigami, 2000, 2001; Asaga et al., 2002). However, glial fibrillary acidic protein (GFAP) was highly susceptible to the attack of PAD2 in excised rat brains deliberately left at room temperature (Asaga and Senshu, 1993). These findings provided a clue that PAD2 normally remains inactive but becomes active and citrullinates cellular proteins when the intracellular calcium balance is upset during neurodegenerative changes.

The pathological presentation of AD involves the selective death of pyramidal neurons and an accumulation of two main abnormal protein aggregates, senile plaques (SPs) and neurofibrillary tangles (NFTs; Katzman, 1986; Smith, 1998). Although NFTs and SPs are found in many areas of the cerebrum, they are concentrated mainly in the hippocampus and cerebral cortex. The former site actually appears to be more important, since pathological indices are first localized in that region (Maccioni et al., 2001). Our previous report indicates that levels of PAD2 are more than threefold higher in the hippocampus than in the cortex of rat brains (Asaga and Ishigami, 2000). Moreover, PAD2 activates and citrullinates various cerebral proteins under hypoxic conditions (Asaga and Ishigami, 2000) and during kainic acid-evoked neurodegeneration (Asaga and Ishigami, 2001; Asaga et al., 2002), suggesting the involvement of protein citrullination in neurodegenerative processes. The present study was therefore designed to test the hypothesis that PAD2 plays a role in AD and that citrullinated proteins are active participants in the neurodegenerative process, particularly in the hippocampus.

MATERIALS AND METHODS

Human Subjects

Brain specimens used in this study were removed at autopsy from 10 patients with AD (seven women and three men) and nine (four women and five men) normal subjects. The subjects' demographic data are summarized in Table I. Specimens were taken from the hippocampus and divided into two parts. One part was fixed with 4% paraformaldehyde and processed for paraffin embedding. Another part was immediately frozen in dry ice. All AD patients met accepted criteria for the neuropathologic diagnosis of AD based on the National Institute of Aging (NIA)-Reagan Institute Criteria for the Neuropathological Diagnosis of AD (1997), combining abundant neuritic plaques in the neocortex (definite AD with Consortium to Establish a Registry for AD Criteria) and a profusion of NFTs in the limbic and neocortical areas (Braak and Braak stage VI). Normal subjects used as controls were individuals with no history of dementia or other neurologic disorders. Neuropathologic evaluation of control brains revealed only age-associated gross and histopathologic alterations (Braak and Braak NFT stage I and senile plaque stage 0 or A). The human studies were approved by the Tokyo Metropolitan Institute of Gerontology (TMIG) Review Boards.

Preparation of Tissue Samples

Frozen hippocampi of AD and control subjects' brains were homogenized in a lysis buffer (0.01 M Tris-HCl, pH 7.6, 1 mM phenylmethylsulfonyl fluoride, 0.1% NP-40) with a Polytron homogenizer. For sodium dodecyl sulfate-polyacrylamide gel electrophoresis (SDS-PAGE), an aliquot of the homogenates was mixed with an equal volume of 0.125 M Tris-HCl, pH 6.8, 4% SDS, 20% glycerol, 10% 2-mercaptoethanol, and 0.005% bromophenol blue (sample buffer) and heated in boiling water for 5 min. The protein content of cell homogenates was measured by the method of Lowry et al. (1951) with bovine serum albumin as a standard.

Detection of Citrullinated Proteins

Citrullinated proteins were detected by Western blotting as described previously (Senshu et al., 1992). Briefly, equal amounts of protein (10 μg/lane) were separated by SDS-PAGE on vertical slab 10% acrylamide gels (1 mm × 9 cm) by the method of Laemmli (1970). Proteins were then electrophoretically transferred from acrylamide gels onto a membrane of poly-

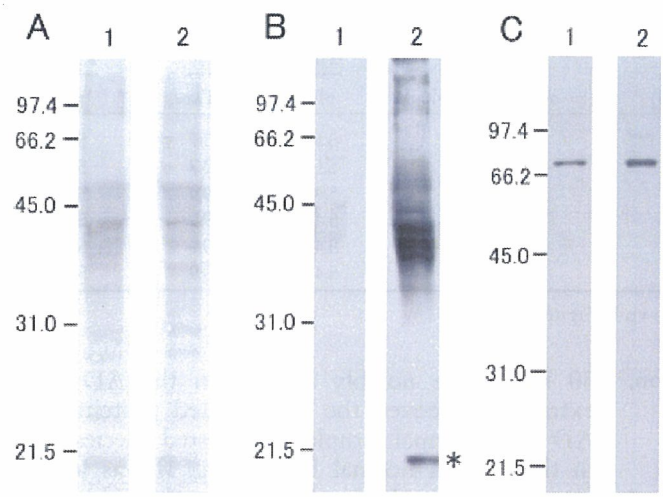

Fig. 1. Western blot analysis of citrullinated proteins and PAD2 in the hippocampus of AD and control brain. Tissue homogenates (10 μg) were separated by SDS-PAGE and transferred to a PVDF membrane. **A:** Typical protein profiles detected by amido black staining. **B:** Citrullinated protein profiles detected as described in Materials and Methods. **C:** Immunoreactive PAD2 profiles. Lane 1, age-matched control; lane 2, AD. Asterisks indicate the citrullinated MBP.

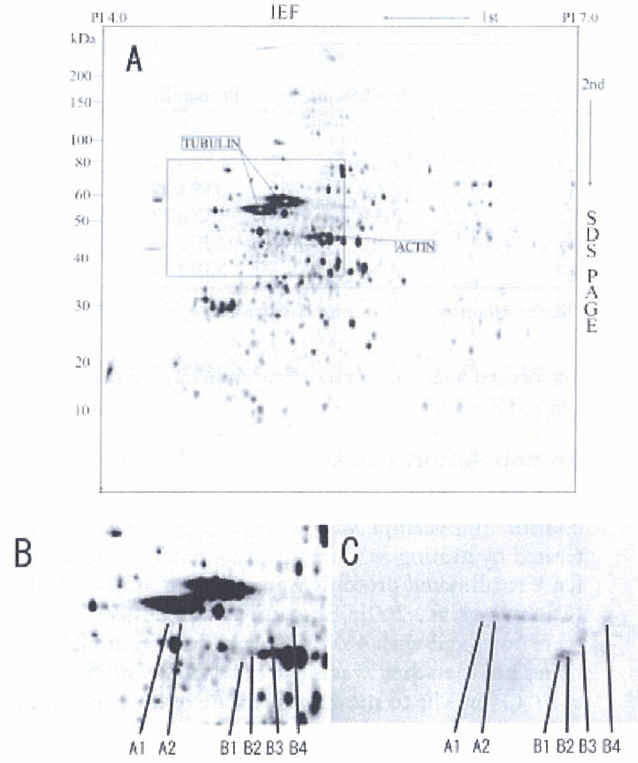

Fig. 2. Proteome analysis of citrullinated proteins in the hippocampus of AD brain. **A:** Two-dimensional protein profiles of the AD hippocampus. Proteins were separated on the basis of pI (x-axis) and molecular mass (y-axis). Spots were visualized with Sypro Ruby gel staining. IEF, isoelectric focusing. Tubulin and actin were identified by peptide mass fingerprinting and a subsequent database search. **B:** Enlarged proteins of AD hippocampus from 2-DE gels indicated as a rectangular area in A. **C:** Western blot analysis of citrullinated proteins from 2-DE gels indicated as rectangular area in A. Numbered spots were identified by mass spectrometry.

vinylidene difluoride (PVDF; Millipore, Billerica, MA) by the method of Towbin et al. (1979). Citrulline residues on the membrane were modified by overnight incubation at 37°C in modification medium [1 volume of 1% diacetyl monoxime/0.5% antipyrine/1 N acetic acid, and two volumes of a mixture of 85% H_3PO_4/98% H_2SO_4/H_2O (20/25/55) containing 0.025% $FeCl_3$]. The membrane was then incubated successively with antimodified citrulline IgG antibody produced in a rabbit and with purified (Senshu et al., 1992), horseradish peroxidase-labeled goat anti-rabbit IgG (Bio-Rad, Hercules, CA). Chemiluminescence signals were detected on Kodak XAR films with ECL Western Blotting Detection Reagents (Amersham Bioscience, Piscataway, NJ).

Two-Dimensional Gel Electrophoresis and Proteome Analysis

Protein extraction and two-dimensional gel electrophoresis (2-DE) were performed as reported previously (Toda et al., 1998; see also http://proteome.tmig.or.jp/2D/2DEmethod.html). Briefly, 100 mg of tissue sample were crushed in liquid nitrogen and lysed with 300 μl of 5 M urea, 2 M thiourea, 2% CHAPS, 2% SB3-10, 1% Pharmalyte (pH 3–10; Amersham Bioscience), 1% dithiothreitol (DTT), and 1% proteinase inhibitor cocktail (Sigma-Aldrich, St. Louis, MO) with sonication. One hundred micrograms of protein were loaded onto gel strips with an immobilized pH gradient (pH 4–7; 18 cm; Amersham Biosciences), and isoelectric focusing was performed on a CoolPhoreStar model 3610 (Anatech, Tokyo, Japan). After isoelectric focusing, strips were equilibrated with 50 mM Tris-HCl, pH 6.8, 6 M urea, 2 M thiourea, 2% SDS, 30% glycerol, and 1% DTT for 30 min and then with the same solution containing 4% iodoacetamide instead of DTT for 30 min. Each equilibrated strip was mounted on a 7.5% SDS-polyacrylamide gel and fixed with shark-tooth combs. SDS-PAGE was performed on a vertical format using a Tricine buffer system. After second-dimension electrophoresis, gels were fixed in 10% methanol and 6% acetic acid for 30 min, and protein spots were visualized by Sypro Ruby (Molecular Probes, Eugene, OR) staining, following the manufacturer's recommendations.

A square (8 × 8 cm) containing tubulin was cut off from the gel slab and then applied to Western blots to detect the citrullinated proteins according to the method described above, because these citrullinated proteins were previously detected at the same position of tubulin on 2-DE using minislab gel (8 × 8 cm). At this time, the citrullinated proteins were detected by using the highly sensitive reagent ECL Advance (Amersham Bioscience). Thereafter, the protein spots visualized with Cypro Ruby and matched with the citrullinated proteins were excised with a ProteomeWorks Spot Cutter (Bio-Rad) followed by in-gel digestion with trypsin according to the manufacturer's specifications. The digested peptide was directly mixed with an equal volume of 10 mg/ml α-cyano-4-hydroxycinnamic acid, and peptide mass spectra were obtained on an AXIMA-CFR MALDI-TOF-MASS (Shimadzu, Kyoto, Japan) platform. Peptide mass mapping was

TABLE II. Proteins Identified From 2-DE Gels of AD Hippocampus by MALDI-TOF Mass Spectrometry

Spot no.[a]	Protein	Probability	Sequence coverage (%)	NCBI accession Nos.	Theoretical value		Experimental value	
					pI	kDa	pI	kDa
A1	Vimentin	3.8E+02	68	CAA39600	5.1	53.7	5.1	49.2
A2	Vimentin	4.3E+02	71	CAA39600	5.1	53.7	5.1	49.1
B1	GFAP	3.1E+02	53	NP_002046	5.4	49.9	5.2	43.5
B2	GFAP	3.3E+02	57	NP_002046	5.4	49.9	5.2	44.8
B3	GFAP	3.2E+02	55	NP_002046	5.4	49.9	5.3	47.4
B4	GFAP	3.3E+02	60	NP_002046	5.4	49.9	5.3	49.9

[a]The numbering and lettering corresponding to the 2-DE gets image shown in Figure 2A.

performed by using Mascot Search (Matrix Science Ltd., London, United Kingdom).

Immunohistochemistry

The paraffin-embedded sections (6-μm-thick) of AD and control hippocampi were deparaffinized, rehydrated, and pretreated by heating in a microwave oven for 10 min in citrate buffer. Citrullinated proteins were detected as described previously (Ohsawa et al., 2001; Ishigami et al., 2002a). Briefly, sections were postfixed with 4% paraformaldehyde and 2.5% glutaraldehyde, and then they were incubated in the modification medium at 37°C for 3 hr to modify citrulline residues in situ. Immunostaining of citrullinated proteins was performed with antimodified citrulline IgG and the Vectastain Elite ABC kit (Vector Laboratories, Burlingame, CA) using 3,3′-diaminobenzidine as a chromogenic substrate. Human PAD2 and GFAP were stained with rabbit anti-human PAD2 prepared as described previously (Ishigami et al., 2002b) and monoclonal antibodies to GFAP (Sigma-Aldrich), respectively. Sections were also subjected to hematoxylin staining for histological examinations. To evaluate the degree of citrullinated protein and PAD2 immunoreactivity, we used a scoring system, in which immunoreactivity was arbitrarily defined from grade 0 (no immunoreactivity detected) to grade 4 (the most intensive immunoreactivity detected). The scores obtained from 10 AD and nine control subjects were then averaged.

The citrullinated proteins, human PAD2 and GFAP, were detected with immunofluorescent labeling and confocal microscopy (LSM-510 laser scanning microscope; Carl Zeiss, Oberkochen, Germany). Primary antibodies were visualized with Alexa Fluor 488 goat anti-rabbit IgG and Alexa Fluor 594 goat anti-mouse IgG (Molecular Probes).

Statistical Analysis

The results are expressed as the mean ± SEM. The probability of statistical differences between experimental groups was determined by a Student's *t*-test, as indicated.

RESULTS

Identification and Characterization of Citrullinated Proteins in the Hippocampi of AD Patients and Normal Controls

Figure 1A shows total proteins in hippocampal extracts from brains of AD and normal individuals in which amido black staining delineated obviously different profiles. In particular, the protein bands between 30 and 50 kDa were notably smaller in the AD hippocampal extracts. Moreover, the citrullinated protein profile from AD hippocampal samples manifested species not detected in those from normal brains (Fig. 1B) as judged by the procedures described in Materials and Methods. In particular, a band migrating at approximately 20 kDa, which was previously shown to be myelin basic protein (MBP) in cultured oligodendrocytes (Akiyama et al., 1999), was present in relatively large quantities in the AD hippocampus but essentially undetectable in this region from normal brains. We confirmed the identity of this protein by immunoprecipitation using specific MBP antiserum (data not shown). Western blots of PAD2 revealed a single band migrating at approximately 75 kDa in hippocampal extracts from both normal and AD brains (Fig. 1C).

AD hippocampal proteins were further characterized by 2-DE (Fig. 2A). Because citrullinated proteins were detected in abundance migrating over 35 kDa, as shown in Figure 1B, the gel region outlined in Figure 2A was cut out (Fig. 2B), and the citrullinated proteins were subjected to Western blotting for identification. Figure 2C shows several of the AD hippocampal citrullinated proteins detected and identification of these proteins by peptide mass fingerprinting and a subsequent database search. These methods identified vimentin as proteins A1 and A2 and GFAP as proteins B1, B2, B3, and B4 (Table II). Some citrullinated proteins were visible throughout the gel (Fig. 2A), even outside the region cut out (data not shown).

Immunohistochemical Localization of Citrullinated Proteins and PAD2 in Hippocampal Regions and Cell Type

Figure 3A shows the regional localization of citrullinated proteins in the hippocampus of an AD brain. Citrullinated proteins were detected throughout the hippocampus, especially in the conjugation region between molecular layers of hippocampus and dentate gyrus as well as polymorphic layers of dentate gyrus and stratum radiatum of CA1 and CA2 areas. No such proteins were found in the granular layer of the dentate gyrus. Moreover, no citrullinated proteins at all were detected in a normal hippocampus (Fig. 3B). A scoring system adopted to evaluate the degree of citrullinated protein immunoreactivity in the hippocampus then revealed significantly greater immunoreactivity in the AD hippocampus than in its normal counterpart (Fig. 4A). In contrast, PAD2 immunoreactivity was detect-

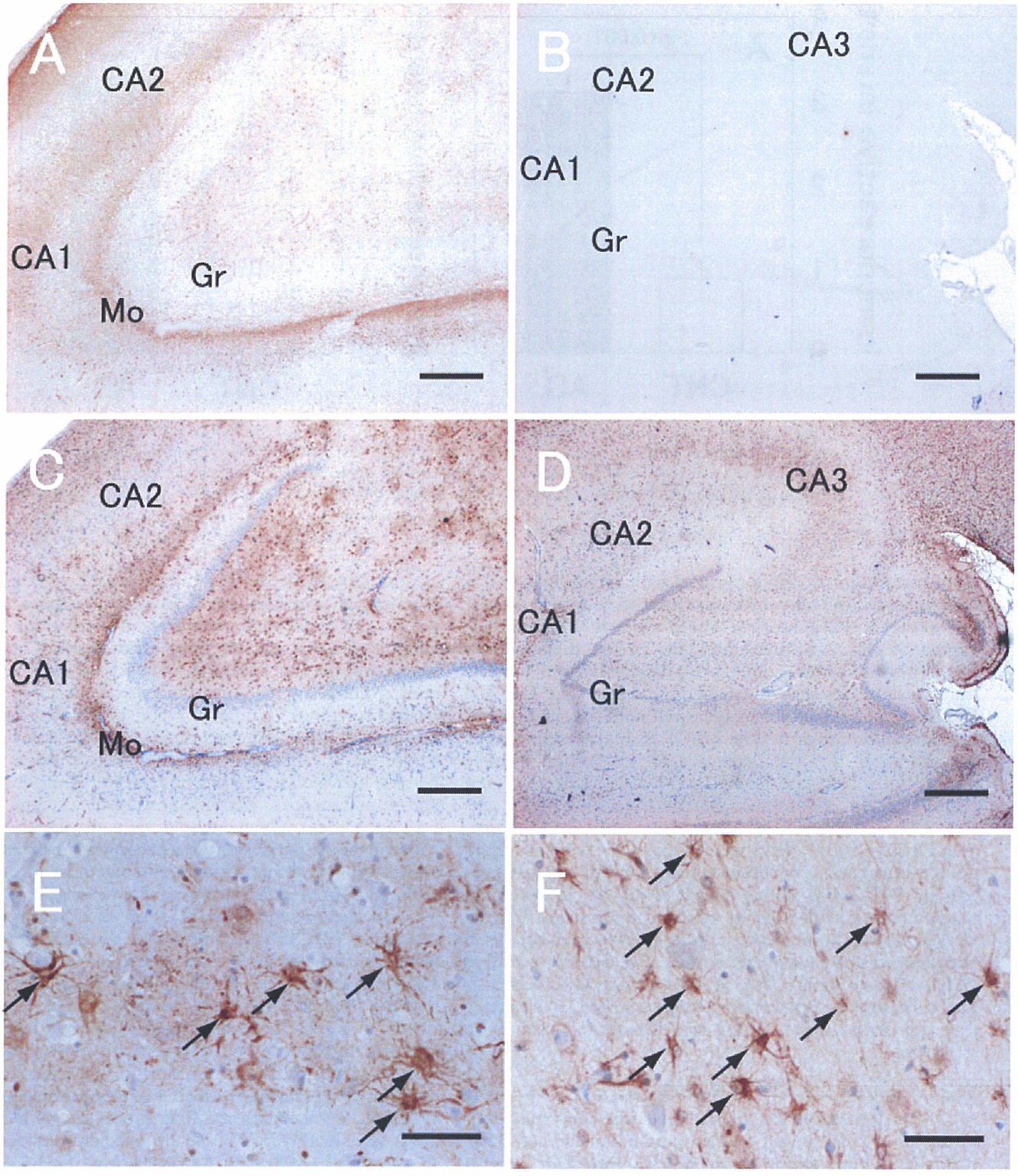

Fig. 3. Immunohistochemical staining of citrullinated proteins and PAD2. Hippocampal sections from AD (**A,C**) and control (**B,D**) brains were stained for citrullinated proteins (A,B) and PAD2 (C,D) as described in Materials and Methods. **E:** Higher magnification of A. Arrows indicate the citrullinated protein-positive cells. **F:** Higher magnification of C. Arrows indicate the PAD2-positive cells. Gr, granule cell layer; Mo, molecular cell layer. Scale bars = 500 μm in A–D, 50 μm in E,F.

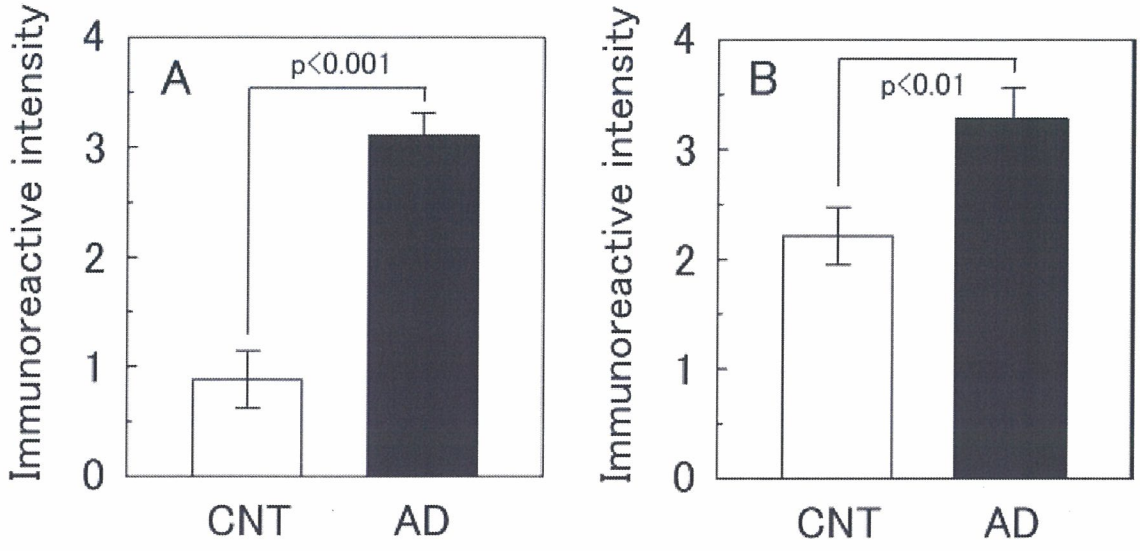

Fig. 4. Immunoreactive intensity of citrullinated proteins and PAD2 in the hippocampi of AD and control brains. The immunoreactivity of citrullinated proteins (**A**) and PAD2 (**B**) in the hippocampus was graded (grade 0 to 4) as described in Materials and Methods. Values are expressed as means ± SEM of 10 AD and nine control subjects. Data were compared by Student's *t*-test.

able all through the hippocampus, both in the AD and in normal brain, but not in the granular layer of the dentate gyrus (Fig. 3C,D). A scoring system adopted to evaluate the degree of PAD2 immunoreactivity in the hippocampus revealed significantly greater immunoreactivity in the AD hippocampus than in its normal counterpart (Fig. 4B). The PAD2-enriched region coincided well with the citrullinated protein-positive regions (Fig. 3A,C). At higher microscopic magnification in the polymorphic layer of dentate gyrus, figures of citrullinated protein-positive cells and PAD2-positive cells were apparent as astrocyte-like cells (Fig. 3E,F). To confirm whether these citrullinated protein- and PAD2-positive cells were astrocytes, we performed double-immunofluorescence staining for citrullinated protein or PAD2 and GFAP, which is an astrocyte-specific marker protein, followed by confocal microscopy (Fig. 5). GFAP-positive fluorescence signals clearly coincided with citrullinated protein-positive signals (Fig. 5A–C) as well as PAD2-positive signals (Fig. 5D–F). Almost all GFAP-positive cells showed immunoreactivity for PAD2, despite a few exceptions. Thus, PAD2 was distributed mainly in astrocytes.

DISCUSSION

We report here, for the first time, the abnormal accumulation of citrullinated proteins and abnormal activation of PAD2 in brain extracts from patients with AD. Citrullinated proteins were barely detectable in normal human brain extracts, although PAD2 was almost universally present.

Previously, we found similar results in the normal rat brain (Asaga and Ishigami, 2000, 2001). Additionally, physiologic insults such as hypoxia and kainic acid administration also resulted in the appearance of citrullinated proteins (Asaga and Ishigami, 2000, 2001; Asaga et al., 2002). PAD2 was present in the rat cerebrum and especially enriched in the dentate gyrus and stratum radiatum of hippocampus, the amygdala, the hypothalamus, and the cortex, but few or no citrullinated proteins were detected in those regions. Under hypoxic conditions (Asaga and Ishigami, 2000) and during kainic acid-evoked neurodegeneration (Asaga and Ishigami, 2001; Asaga et al., 2002), PAD2 became activated in regions undergoing neurodegeneration and functioned to citrullinate various cerebral proteins, indicating the involvement of protein citrullination in neurodegenerative processes. We are convinced that these past and present results confirm the involvement of protein citrullination in human neurodegenerative disease.

In the present study, Western blot analysis revealed numerous citrullinated proteins in the AD hippocampus. We identified citrullinated vimentin and GFAP, which were shown as several independent spots by 2-DE and proteomic analysis (Fig. 2C, Table II). Because protein citrullination results in a decrease in the net positive charge of proteins, each spot must be shown as several pI values with different degrees of citrullination resulting in neutralization of proteins. In the epidermis of mice, we previously identified citrullinated cytokeratins and filaggrin as several independent spots separable by 2-DE and detected by Western blotting (Senshu et al., 1995, 1999). Citrullination of cytokeratins and filaggrin occurs during the latest stages of epidermal differentiation and is thought to play a key role in the cornification process (Senshu et al., 1995). Although citrullination of vimentin and GFAP seems to be much more specific than that of other intracellular proteins, it is still unclear whether citrullination of vimentin and GFAP has physiologically

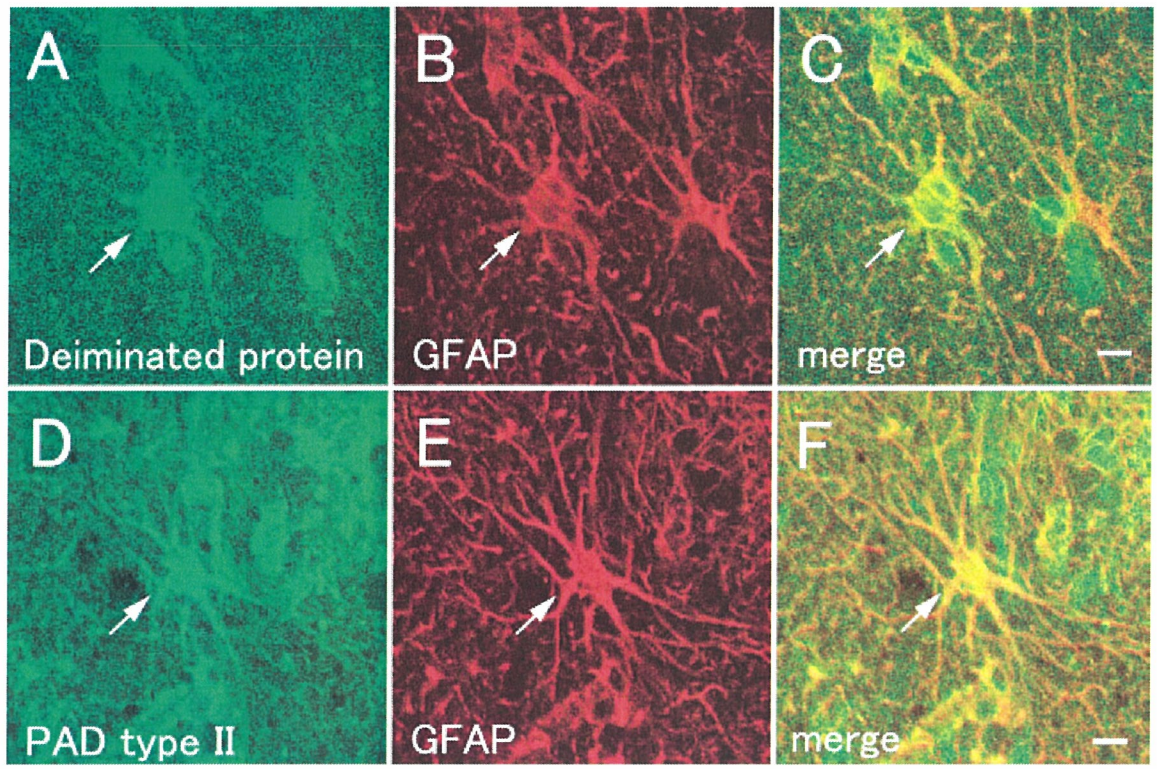

Fig. 5. Identification of citrullinated protein-positive and PAD2-positive cells by double immunofluorescence staining. Sections of AD hippocampus were doubly immunostained with monoclonal anti-GFAP antibody and with polyclonal antimodified citrulline IgG or polyclonal anti-human PAD2 antibody. The primary antibodies were visualized with anti-rabbit Alexa Fluor 488 (green) and anti-mouse Alexa Fluor 594 (red). **A,D:** Alexa 488 (green) for citrullinated protein (A) or PAD2 (D). **B,E:** Alexa 568 (red) for GFAP. **C,F:** Merged views for A/B and D/E, respectively. Arrows indicate coincident position. Scale bars = 5 μm.

important functions in the brains of AD patients. Inagaki et al. (1989) reported that vimentin and GFAP were highly susceptible to the attack of PAD2 in vitro; for example, citrullination of vimentin induced disassembly of intermediate filaments.

Here, we also identified citrullinated MBP, which is an authentic marker of oligodendrocyte, in the AD-afflicted hippocampus. Recently, we found PAD2 localized in a stage-specific, immature oligodendrocyte from a rat's cerebral hemisphere in vitro (Akiyama et al., 1999). Gould et al. (2000) reported that PAD2 cDNA was highly expressed in myelin sheath assembly sites with a combination of subcellular fractionation and suppression subtractive hybridization. Moreover, Moscarello et al. (1994, 2002) reported that PAD enzyme and citrullinated MBP are relatively enriched in immature myelin and that MBP citrullination has an important role in myelin development and in the human demyelinating disease multiple sclerosis. Recently, many investigators have suggested that myelin breakdown may be a contributing factor in the pathology of AD (Bartzokis, 2004; Tian et al., 2004). MBP citrullination might also contribute to the myelin breakdown.

The mechanism(s) by which citrullinated proteins occur in the hippocampus during AD remains unclear. Possibly PAD2 becomes activated, abundant, and functional only in the presence of AD, insofar as the amount of PAD2 increased notably in hippocampi of the AD patients we assessed compared with that in normal subjects. Although PAD2 was also present in hippocampal extracts from normal subjects, that enzyme remained in a steady state during which no enzyme activation occurred. For enzyme activation, the intracellular calcium concentration must become elevated. No other factors can regulate PAD activity in vivo or in vitro, to the best of our knowledge. A loss of neuronal calcium homeostasis leading to increases in the intracellular calcium concentration has been proposed to play a major role in hypoxic and ischemic brain injury (Choi, 1988; Hossmann, 1999). Haun et al. (1992) suggested that an influx of extracellular calcium contributes to astroglial injury during ischemia on the basis of their experimental results with simulated ischemia in a primary culture of astrocytes. Our previous report showed that PAD2 activated and citrullinated various cerebral proteins under hypoxic conditions (Asaga and Ishigami, 2000) and during kainic acid-evoked neurodegeneration (Asaga and Ishigami, 2001; Asaga et al., 2002). Abnormal PAD activation resulted in random protein citrullination, which could then trigger the onset of neurodegenerative disease.

In conclusion, the present data indicate that patients with AD bear an abnormal accumulation of citrullinated

proteins and abnormal activation of PAD2 in the hippocampus. Therefore, citrullinated proteins may be a useful marker for neurodegenerative disease. Moreover, the development of an inhibitory drug specific for PAD2 could conceivably prevent the onset and progression of neurodegeneration.

ACKNOWLEDGMENTS

The excellent editorial assistance of Ms. P. Minick is gratefully acknowledged. This study was supported by a Grant-in-Aid for Scientific Research from the Ministry of Education, Science, and Culture, Japan (to A.I.) and a grant from Health Science Research Grants for Comprehensive Research on Aging and Health supported by the Ministry of Health Labor and Welfare, Japan (to A.I.). Additional support was provided by the SHISEIDO Grant for Scientific Research (to A.I.), the Cosmetology Research Foundation (to A.I.), and the Nakatomi Foundation (to A.I.).

REFERENCES

Akiyama K, Sakurai Y, Asou H, Senshu T. 1999. Localization of peptidylarginine deiminase type II in a stage-specific immature oligodendrocyte from rat cerebral hemisphere. Neurosci Lett 274:53–55.

Asaga H, Ishigami A. 2000. Protein deimination in the rat brain: generation of citrulline-containing proteins in cerebrum perfused with oxygen-deprived media. Biomed Res 21:197–205.

Asaga H, Ishigami A. 2001. Protein deimination in the rat brain after kainate administration: citrulline-containing proteins as a novel marker of neurodegeneration. Neurosci Lett 299:5–8.

Asaga H, Senshu T. 1993. Combined biochemical and immunocytochemical analyses of postmortem protein deimination in the rat spinal cord. Cell Biol Int 17:525–532.

Asaga H, Akiyama K, Ohsawa T, Ishigami A. 2002. Increased and type II-specific expression of peptidylarginine deiminase in activated microglia but not hyperplastic astrocytes following kainic acid-evoked neurodegeneration in the rat brain. Neurosci Lett 326:129–132.

Bartzokis G. 2004. Age-related myelin breakdown: a developmental model of cognitive decline and Alzheimer's disease. Neurobiol Aging 25: 5–18.

Chavanas S, Mechin MC, Takahara H, Kawada A, Nachat R, Serre G, Simon M. 2004. Comparative analysis of the mouse and human peptidylarginine deiminase gene clusters reveals highly conserved non-coding segments and a new human gene, PADI6. Gene 330:19–27.

Choi DW. 1988. Calcium-mediated neurotoxicity: relationship to specific channel types and role in ischemic damage. Trends Neurosci 11:465–469.

Gould RM, Freund CM, Palmer F, Feinstein DL. 2000. Messenger RNAs located in myelin sheath assembly sites. J Neurochem 75:1834–1844.

Haun SE, Murphy EJ, Bates CM, Horrocks LA. 1992. Extracellular calcium is a mediator of astroglial injury during combined glucose-oxygen deprivation. Brain Res 593:45–50.

Hossmann KA. 1999. The hypoxic brain. Insights from ischemia research. Adv Exp Med Biol 474:155–169.

Imparl JM, Senshu T, Graves DJ. 1995. Studies of calcineurin-calmodulin interaction: probing the role of arginine residues using peptidylarginine deiminase. Arch Biochem Biophys 318:370–377.

Inagaki M, Takahara H, Nishi Y, Sugawara K, Sato C. 1989. Ca^{2+}-dependent deimination-induced disassembly of intermediate filaments involves specific modification of the amino-terminal head domain. J Biol Chem 264:18119–18127.

Ishigami A, Ohsawa T, Watanabe K, Senshu T. 1996. All-trans retinoic acid increases peptidylarginine deiminases in a newborn rat keratinocyte cell line. Biochem Biophys Res Commun 223:299–303.

Ishigami A, Kuramoto M, Yamada M, Watanabe K, Senshu T. 1998. Molecular cloning of two novel types of peptidylarginine deiminase cDNAs from retinoic acid-treated culture of a newborn rat keratinocyte cell line. FEBS Lett 433:113–118.

Ishigami A, Asaga H, Ohsawa T, Akiyama K, Maruyama N. 2001. Peptidylarginine deiminase type I, type II, type III and type IV are expressed in rat epidermis. Biomed Res 22:63–65.

Ishigami A, Asaga H, Ohsawa T, Akiyama K, Maruyama N. 2002a. Protein deimination and peptidylarginine deiminase expression during cornification of rat epidermal keratinocytes. Biomed Res 23:145–151.

Ishigami A, Ohsawa T, Asaga H, Akiyama K, Kuramoto M, Maruyama N. 2002b. Human peptidylarginine deiminase type II: molecular cloning, gene organization, and expression in human skin. Arch Biochem Biophys 407:25–31.

Katzman R. 1986. Alzheimer's disease. N Engl J Med 314:964–973.

Keller JN, Hanni KB, Markesbery WR. 2000. Impaired proteasome function in Alzheimer's disease. J Neurochem 75:436–439.

Kubilus J, Baden HP. 1983. Purification and properties of a brain enzyme which deiminates proteins. Biochim Biophys Acta 745:285–291.

Kubilus J, Waitkus RF, Baden HP. 1980. Partial purification and specificity of an arginine-converting enzyme from bovine epidermis. Biochim Biophys Acta 615:246–251.

Laemmli UK. 1970. Cleavage of structural proteins during the assembly of the head of bacteriophage T4. Nature 227:680–685.

Lamensa JW, Moscarello MA. 1993. Deimination of human myelin basic protein by a peptidylarginine deiminase from bovine brain. J Neurochem 61:987–996.

Lowry OH, Rosebrough NJ, Farr AL, Randall RJ. 1951. Protein measurement with the phenol reagent. J Cell Biol 193:265–275.

Maccioni RB, Munoz JP, Barbeito L. 2001. The molecular bases of Alzheimer's disease and other neurodegenerative disorders. Arch Med Res 32:367–381.

Moscarello MA, Wood DD, Ackerley C, Boulias C. 1994. Myelin in multiple sclerosis is developmentally immature. J Clin Invest 94:146–154.

Moscarello MA, Pritzker L, Mastronardi FG, Wood DD. 2002. Peptidylarginine deiminase: a candidate factor in demyelinating disease. J Neurochem 81:335–343.

Nakashima K, Hagiwara T, Ishigami A, Nagata S, Asaga H, Kuramoto M, Senshu T, Yamada M. 1999. Molecular characterization of peptidylarginine deiminase in HL-60 cells induced by retinoic acid and 1α, 25-dihydroxyvitamin D_3. J Biol Chem 274:27786–27792.

National Institute on Aging, and Reagan Institute Working Group on Diagnostic Criteria for the Neuropathological Assessment of Alzheimer's Disease. 1997. Consensus recommendations for the postmortem diagnosis of Alzheimer's disease. Neurobiol Aging 18:S1–S2.

Nishijyo T, Kawada A, Kanno T, Shiraiwa M, Takahara H. 1997. Isolation and molecular cloning of epidermal- and hair follicle-specific peptidylarginine deiminase (type III) from rat. J Biochem (Tokyo) 121:868–875.

Ohsawa T, Ishigami A, Akiyama K, Asaga H. 2001. Immunocytochemical localization of peptidylarginine deiminase type III, trichohyalin and deiminated trichohyalin in infant rat dorsal skin hair follicle. Biomed Res 22:91–97.

Rogers GE, Simmonds DH. 1958. Content of citrulline and other amino acids in a protein of hair follicles. Nature 182:186–187.

Rus'd AA, Ikejiri Y, Ono H, Yonekawa T, Shiraiwa M, Kawada A, Takahara H. 1999. Molecular cloning of cDNAs of mouse peptidylarginine deiminase type I, type III and type IV, and the expression pattern of type I in mouse. Eur J Biochem 259:660–669.

Senshu T, Sato T, Inoue T, Akiyama K, Asaga H. 1992. Detection of citrulline residues in deiminated proteins on polyvinylidene difluoride membrane. Anal Biochem 203:94–100.

Senshu T, Akiyama K, Kan S, Asaga H, Ishigami A, Manabe M. 1995. Detection of deiminated proteins in rat skin: probing with a monospecific antibody after modification of citrulline residues. J Invest Dermatol 105:163–169.

Senshu T, Akiyama K, Ishigami A, Nomura K. 1999. Studies on specificity of peptidylarginine deiminase reactions using an immunochemical probe that recognizes an enzymatically deiminated partial sequence of mouse keratin K1. J Dermatol Sci 21:113–126.

Smith MA. 1998. Alzheimer disease. Int Rev Neurobiol 42:1–54.

Tarcsa E, Marekov LN, Mei G, Melino G, Lee S-C, Steinert PM. 1996. Protein unfolding by peptidylarginine deiminase. Substrate specificity and structural relationships of the natural substrates trichohyalin and filaggrin. J Biol Chem 271:30709–30716.

Terakawa H, Takahara H, Sugawara K. 1991. Three types of mouse peptidylarginine deiminase: characterization and tissue distribution. J Biochem (Tokyo) 110:661–666.

Tian J, Shi J, Bailey K, Mann DM. 2004. Relationships between arteriosclerosis, cerebral amyloid angiopathy and myelin loss from cerebral cortical white matter in Alzheimer's disease. Neuropathol Appl Neurobiol 30:46–56.

Toda T, Kaji K, Kimura N. 1998. TMIG-2DPAGE: a new concept of two-dimensional gel protein database for research on aging. Electrophoresis 19:344–348.

Towbin H, Staehelin T, Gordon J. 1979. Electrophoretic transfer of proteins from polyacrylamide gels to nitrocellulose sheets: procedure and some applications. Proc Natl Acad Sci U S A 76:4350–4354.

Tsuchida M, Takahara H, Minami N, Arai T, Kobayashi Y, Tsujimoto H, Fukazawa C, Sugawara K. 1993. cDNA nucleotide sequence and primary structure of mouse uterine peptidylarginine deiminase. Detection of a 3′-untranslated nucleotide sequence common to the mRNA of transiently expressed genes and rapid turnover of this enzyme's mRNA in the estrous cycle. Eur J Biochem 215:677–685.

Vincent SR, Leung E, Watanabe K. 1992. Immunohistochemical localization of peptidylarginine deiminase in the rat brain. J Chem Neuroanat 5:159–168.

Watanabe K, Senshu T. 1989. Isolation and characterization of cDNA clones encoding rat skeletal muscle peptidylarginine deiminase. J Biol Chem 264:15255–15260.

Watanabe K, Akiyama K, Hikichi K, Ohtsuka R, Okuyama A, Senshu T. 1988. Combined biochemical and immunochemical comparison of peptidylarginine deiminases present in various tissues. Biochim Biophys Acta 966:375–383.

Kidney International, Vol. 68 (2005), pp. 84–95

Citrullination preferentially proceeds in glomerular Bowman's capsule and increases in obstructive nephropathy

DONGYUN FENG, TOSHIYUKI IMASAWA, TADASUKE NAGANO, MASARU KIKKAWA, KAORI TAKAYANAGI, TAKAKO OHSAWA, KYOICHI AKIYAMA, AKIHITO ISHIGAMI, TOSIFUSA TODA, TETSUYA MITARAI, TAKEO MACHIDA, and NAOKI MARUYAMA

Department of Molecular Pathology, Tokyo Metropolitan Institute of Gerontology, Tokyo, Japan; Department of Bioactivity Regulation, Tokyo Metropolitan Institute of Gerontology, Tokyo, Japan; Department of Proteome Analysis, Tokyo Metropolitan Institute of Gerontology, Tokyo, Japan; Department of Internal Medicine and Division of Immunopathology, Clinical Research Center, Chiba-East National Hospital, Chiba, Japan; Division of Nephrology, Saitama Medical Center, Saitama Medical School, Saitama, Japan; and Department of Regulation Biology, Faculty of Science, Saitama University, Saitama, Japan

Citrullination preferentially proceeds in glomerular Bowman's capsule and increases in obstructive nephropathy.

Background. Peptidylarginine deiminases (PADs) are a group of posttranslational modification enzymes that citrullinate (deiminate) protein arginine residues, yielding citrulline residues. Citrullination of arginine residues abolishes their positive charge, markedly altering their structure. We undertook this study to investigate the actions of PADs in the kidney.

Methods. In male rats, we ligated the unilateral ureter, then analyzed the obstructed and contralateral kidneys 1 week later. Controls were rats simultaneously given sham operations. In another experiment, we ligated unilateral ureters of eight rats, four of which received a ureter-bladder anastomosis 1 week later. These rats were subjected to histologic examinations 5 weeks after unilateral ureteral obstruction (UUO).

Results. Reverse transcription-polymerase chain reaction (RT-PCR) revealed that, of PADs (type I, II, III, and IV), only PAD type II was expressed in kidneys. Western blot study showed that PAD type II expression and citrullinated protein content increased greatly in kidneys that underwent unilateral ureteral ligation compared to that in contralateral or sham-operated kidneys. Immunohistochemical analyses revealed that PAD type II was preferentially expressed by parietal epithelial cells and that only in Bowman's capsule were proteins citrullinated. Additionally, these PAD type II and citrullinated proteins in obstructed nephropathy were significantly attenuated by the release of the obstruction. Proteome analysis revealed that one of citrullinated proteins in the kidney should be actin.

Conclusion. This result indicates that PAD type II and citrullinated proteins are suitable markers of Bowman's capsule. Not only are these markers preferentially expressed in Bowman's capsules but their expression is also increased in damaged kidneys by UUO, features that promise the further clarification of kidney diseases.

Key words: obstructive nephropathy, Bowman's capsule, parietal epithelial cells, citrullination, peptidylarginine deiminases (PAD), posttranslational modification.

Received for publication August 26, 2004
and in revised form December 7, 2004, and January 15, 2005
Accepted for publication January 28, 2005

Bowman's capsule, the outer epithelial wall of the glomerular corpuscle, surrounds glomeruli's loops and lobules. In normal conditions, parietal epithelial cells constituting Bowman's capsule are simple, flat squamous structures. However, the conformation of parietal epithelial cells variously changes in response to such pathologic stimuli as ischemia, hypertension, and inflammation. The result is thickening of the parietal epithelium, and as these parietal epithelial cells proliferate, they become cuboidal and form the glomerular crescents that typify some types of glomerulonephritis. Although Bowman's capsule frequently develops this conformation in patients with kidney diseases, few studies have dealt with it. To date, protein gene product 9.5 is the only known specific marker for Bowman's capsule but this also localizes nerve fibers around arteries [1].

Peptidylarginine deiminase (PADs) are posttranslational modification enzymes that convert protein arginine to citrulline residues [2, 3]. Enzymatic citrullination (deimination) abolishes the positive charge of protein molecules inevitably causing significant alterations in their structure and function [4, 5]. These PADs are distinct from nitric oxide synthetase (NOS) and arginine deiminase, which convert free arginine to citrulline. Mammals have four types of PADs, designated as type I, type II, type III, and type IV [6]. Functionally, PADs have been linked with the pathogenesis of some diseases; for example, PAD type IV is the proposed cause of rheumatoid arthritis and multiple sclerosis [4, 7–9].

Multiple mammalian tissues contain PADs [10] and PAD expression has tissue specificity; for examples, although all PADs are present in epidermis [6], only PAD type II is exclusively expressed in brain [9]. Moreover, citrullination by all PADs shows a definite requirement for Ca^{2+} [11]. Although the mRNA of PAD type II and type IV was previously identified in the rat kidney [6], whether citrullinated proteins also occupy the kidneys

remains uncertain. Therefore, in this study, we used a rat model of kidneys damaged by unilateral ureteral obstruction (UUO) to assess the expression of PADs and the presence of citrullinated proteins. As a result, we present here the first report that specific markers are preferentially expressed in glomerular Bowman's capsules of the kidney and that their expression increases in response to kidney damage.

METHODS

Animals

Male Sprague-Dawley rats (Charles River Breeding Laboratories, Wilmington, MA, USA), weighing 150 to 180 g, were used in this study. Animals were fed standard rodent chow and were given water ad libitum. After intraperitoneal administration of pentobarbital (5.0 mg/kg body weight) (Dainippon Pharmaceutical Co., Ltd, Osaka, Japan), anesthetized animals underwent either left proximal ureteral ligation ($N = 6$) or, simultaneously, a sham operation ($N = 6$). One week later, the obstructed (left UUO) kidneys and the contralateral unobstructed (right) kidneys as well as normal kidneys from sham-operated animals were harvested from these rats. Before removal, the kidneys were well perfused with approximately 100 mL of normal saline to remove circulating blood cell fractions or adherent cells. Blood samples were centrifuged (6000 rpm for 3 minutes) to separate serum for biochemical measurements. Blood urea nitrogen (BUN) and serum creatinine were measured by urease-ultraviolet and enzymatic reaction, respectively (SRL, Inc., Tokyo Japan).

Ureter-bladder anastomosis

In another animal experiment, eight male Sprague-Dawley rats (150 to 180 g) were subjected to left UUO. Four rats of them underwent operation to make ureter-bladder anastomosis 1 week after the ureteral ligation. For building the anastomosis, a sterile and nontoxic polyethylene tube (external diameter 1 mm) (PE-90) (Clay Adams Intradermic Inc., Sparks, MD, USA) was inserted to dilated left ureter and the bladder and fixed securely by silk ligation. These rats were histologically analyzed 5 weeks after the first UUO operation. Simultaneously, the other four rats with UUO for 5 weeks were examined.

Reverse transcriptase-polymerase chain reaction (RT-PCR)

The kidney cortex was dissected and homogenized in Isogen (Nippon Gene, Tokyo, Japan) to isolate total RNA, followed by treatment with RNase-free DNase I (Nippon Gene) to remove DNA contamination according to the supplier's protocol. The amount of RNA extracted was estimated by spectrophotometer. RT-PCR was performed with a Takara mRNA Selective PCR Kit (Takara Shuzo Co., Ltd., Kyoto, Japan) according to the manufacturer's instructions. RT was performed using antisense oligonucleotide primers. The primers of rat PADs type I, type II, type II, type IV, and glyceraldehyde-3-phosphate dehydrogenase (GAPDH) were designed as described previously [6]. The sense and antisense primers were for rat PAD type I, 5′-AGGTATTAGAA GATGGTGGGGTAGG-3′ and 5′-CCCAACCTTCTC ATCCCCCTTTA-3′ (expected size 631 bp) [12]; for rat PAD type II, 5′-ATTCAAGATAGACCAGGAGGA CCAG-3′ and 5′-CAGAATAGGAAGGCCAGTGTCA GAA-3′ (expected size 428 bp) [10]; for rat PAD type III, 5′- CCTTGGCTTGTGCTTCCTATGGT-3′ and 5′-TCCCTCCCTTCTCCCAGTATGTG-3′ (expected size 648 bp) [6]; for rat PAD type IV, 5′-CGCTC CTGGCAGCCTCCCTCGAGGA-3′ and 5′-CAGCAT CTCTAAGCAGGACTGAGTT-3′ (expected size 205 bp) [12]; and for rat GAPDH, 5′-GTGAAGGTCGGT GTGAACGGAT-3′ and 5′-GCCGCCTGCTTCACCAC CTTCTT-3′ (expected size 788 bp) [6]. We also followed PCR conditions as reported with some modifications [6]; 30 minutes at 50°C, and then 15 minutes at 95°C, followed by 31 or 32 cycles at 94°C for 30 seconds, 60°C for 30 seconds, and 72°C for 1 minute, and a terminal extension (72°C, 10 minutes). We used the same templates from each experimented kidney for RT-PCR. The condition of templates was checked by amplification for GAPDH. A positive control for RT-PCR of PADs was obtained from rat epidermis where all PADs are expressed [6]. For RT-PCR of PAD type II, mRNA was amplified by mixing primers of PAD type II and GAPDH. PCR products were visualized by agarose gel electrophoresis with ethidium bromide staining. Bands were quantified by densitometry. GAPDH mRNA was analyzed as an internal control, and relative amounts of PAD type II expression were calculated.

Extraction of proteins and Western blotting

Specimens from the renal cortex containing ~500 mg of protein were sonicated in extraction buffer [20 mmol/L Tris-HCl, 150 mmol/L NaCl, 2 mmol/L ethylenediaminetetraacetic acid (EDTA), 1% Nonidet P40, 50 mmol/L NaF, and 1 mmol/L Na_3VO_4] with protease inhibitor cocktail (Roche, Mannheim, Germany) to extract proteins. Insoluble materials were removed by centrifugation at 15,000 rpm for 10 minutes. The supernatants of samples were incubated with the sample buffer [125 mmol/L Tris-HCl, pH 6.8, 20% glycerol, 10% 2-mercaptoethanol, 4% sodium dodecyl sulfate (SDS), 0.005% bromophenol blue (BPB), and 0.005% methylene blue] and heated in boiling water for 5 minutes. Protein concentrations were estimated with

the BCA Protein Assay Reagent Kit (Pierce, Rockford, IL, USA). Aliquots (30 μg of crude kidney homogenate) were resolved by SDS-polyacrylamide gel electrophoresis (PAGE) (10% gel) and transferred to polyvinylidene difluoride (PVDF) membranes (Millipore, Bedford, MA, USA). The membranes were blocked with 5% nonfat dried milk in Tris-bufferd saline (100 mmol/L Tris-HCl/1.4 mol/L NaCl, pH 7.5)/0.1% Tween-20 (TBST) for 1 hour at room temperature before reaction with the first antibodies. For detection of PAD type II, the blot was incubated with rabbit antirat PAD type II antiserum (×2000) [13]. As a control, the other membrane was incubated with the same concentration of rabbit serum instead of anti PAD type II antibody. For detection of deiminated proteins, we followed a previously reported protocol [14]. Briefly, citrulline residues on the blot were chemically modified by overnight incubation at 37°C in 0.0125% $FeCl_3$, 2.3 mol/L H_2SO_4, 1.5 mol/L H_3PO_4, 0.25% diacetyl monoxime, 0.125% antipyrine, and 0.25 mol/L acetic acid (modification medium). As a control, the other membrane was incubated in the medium free from diacetyl monoxime and antipyrine. The blot was then incubated with a monospecific IgG to modified citrulline (0.125 g/mL) [14]. After reaction with the first antibody, the bound antibodies were detected using horseradish peroxidase–conjugated goat anti-rabbit IgG (PAD type II ×5000, citrulline ×10000) (Bio-Rad Laboratories, Hercules, CA, USA) and enhanced cheminluminescence (ECL) Western blotting detection reagents (Amersham Biosciences Corp., Piscataway, NJ, USA) according to the manufacturer's instructions. To visualize total proteins, Coomassie brilliant blue (CBB) staining was then performed with a Quick-CBB kit (Wako Pure Chemical Industries, Ltd., Osaka, Japan). The bands of PAD type II proteins were quantified by densitometry. The intensity of each band was standardized by the mean of sham-operated group.

Light microscopy

One week after the operation, we performed histologic analyses of the kidneys, which had been sufficiently perfused for removal of circulating cells from the glomeruli. For light microscopy, tissue samples were then fixed with 3% formalin-phosphate-buffered saline (PBS) and embedded in paraffin. After sectioning, the tissues were stained with periodic acid-methenamine-silver (PAM).

PAD staining

Tissue samples from the rats were embedded in 22-oxacalcitriol (OCT) compound (Miles Scientific, Naperville, IL, USA), and quickly frozen in dry ice-acetone. Cryostat sections (4 μm) were fixed in cold acetone for 10 minutes. PAD type II was visible after staining for the indirect fluorescent method. After being washed with PBS, the sections were incubated with rabbit anti-PAD type II antiserum [13], followed by rinsing in PBS and incubation at 37°C for 60 minutes with rhodamine-conjugated sheep antirabbit IgG antibody (ICN Pharmaceuticals, Inc., Aurora, OH, USA). As controls, the tissues were incubated with rabbit serum instead of the first antibody. The sections were rinsed again in PBS, mounted with SlowFade antifade kits (Molecular Probes, Eugene, OR, USA). No positive staining occurred in control tissues. The degrees of PAD type II staining were calculated by two methods. At first, we counted the number of positive glomeruli and expressed them as the percentage of all visible glomeruli. In addition, the area positive for PAD type II in the whole Bowman's capsule of a glomerulus was scored semiquantitatively from 0 to 4: 0, negative staining; 1, less than 25%; 2, 25% to 50%; 3, 50% to 75%; and 4, 75% to 100%. We evaluated more than 30 glomeruli a section and calculated mean value of each section.

Detection of citrullinated protein in situ

Immunostaining of citrullinated proteins was performed by using antimodified citrulline IgG monoclonal antibody and a Vectastain Elite ABC kit (PK-6101) (Vector Laboratories, Inc., Burlingame, CA, USA) as described previously [15]. This antibody reacts with citrulline residues that are chemically modified. Briefly, cryosections were post-fixed with 2.5% glutaraldehyde in PBS and then incubated in the modification medium (0.0125% $FeCl_3$, 2.3 mol/L H_2SO_4, 1.5 mol/L H_3PO_4, 0.25% diacetyl monoxime, 0.125% antipyrine, and 0.25 mol/L acetic acid) at 37°C overnight to modify citrulline residues in situ. Control sections were incubated in the medium free from diacetyl monoxime and antipyrine. After washing with PBS, the sections were incubated with 2% bovine serum albumin (BSA)-PBS at room temperature for 30 minutes to block nonspecific reactions. Then, they were reacted with anti-modified citrulline antibody at 37°C for 2 hours. After washing with PBS, the sections were next incubated with biotinylated antirabbit antibody (Vector Laboratories, Inc) at room temperature for 30 minutes. The sensitivity of this immunostaining was amplified by Elite ABC mixture. Finally, we incubated sections in a peroxidase substrate solution made from buffered substrate for liquid diaminobenzidine (DAB) (Dako Corporation, Carpinteria, CA, USA) and liquid DAB chromogen (Dako Corporation) until the desired stain intensity developed. Staining intensity of citrullinated proteins were analyzed by same ways as scoring of PAD type II staining.

Preparation of protein and two-dimensional gel electrophoresis

Proteins in the kidney were extracted with extraction buffer (8.5 mol/L urea, 0.2% SDS, 2% Triton X-100, 3% 2-mercaptoethanol, 0.8% pharmalyte 3-10, 1 mmol/L Na_3VO_4, and protease inhibitor cocktail), homogenized and centrifuged for 10 minutes at 15,000 rpm. The cytosolic fraction (supernatant) was separated by two dimensional electrophoresis performed in an immobilized pH gradients (IPG)-isoelectric focusing (IEF)/SDS-PAGE system according to the standard protocol found on the Web page *http://proteome.tmig.or.jp/2D/2DE_method.html* with minor modification. In brief, IEF was performed on IPG, pH 4 to 7, 180 mm (Amersham Biosciences AB, Uppsala, Sweden)] with CoolPhorestar model 3610 Horizontal IEF apparatus (Anatech, Tokyo, Japan). The IPG gels were incubated in rehydrating buffer [6 mol/L urea, 2 mol/L thiourea, 13 mmol/L dithiothreitol (DTT), 0.8% pharmalyte 3-10, 2.5 mmol/L acetic acid, 0.0025% (wt/vol) orangeG, and 2% (vol/vol) Triton X-100] overnight. The protein samples (100 μg) were absorbed in a small piece of filter paper and they were applied near the cathode wick on the IPG gel. After 600 to 700 V/hour at 20°C of electrofocusing, the IPG gels were incubated for 30 minutes in equilibration buffer [6 mol/L urea, 33 mmol/L DTT, 25 mmol/L Tris-HCl (pH6.8), 2% (wt/vol) SDS, 0.0025% (wt/vol) BPB, and 30% (vol/vol) glycerol], followed by a 20-minute incubation in equilibration buffer [25 mmol/L Tris-HCl, pH 6.8, 2% (wt/vol) SDS, 0.0025% (wt/vol) BPB, 30% (vol/vol) glycerol, and 0.243 mol/L idoacetamide].

Separation of the second dimension was performed in precast 7.5% SDS/polyacrylamide gel [Tris/Tricine, 200 × 200mm (Anatech)] using the CoolPhoreStar SDS-PAGE Dual-200 vertical slab gel electrophoresis apparatus (Anatech). SDS-PAGE was carried out at 25 mA per gel for 5 hours. After electrophoresis, proteins were stained with Sypro ruby gel stain (Molecular Probes, Inc.) following the manufacturer's protocol and visualized by Molecular Imager FX (Bio-Rad, Tokyo, Japan).

Mass spectrometry

Protein spots exicised from two-dimensional electrophoresed gels were destained and subjected to digestion with sequence-grade modified trypsin (Sigma Chemical Co., St. Louis, MO, USA) at 30°C overnight. The digested peptides was mixed with equal volumes of matrix (10 mg/mL a-cyano-4-hydroxy-trans-cinnamic acid in 50% acetonitrile, 40% methanol, and 0.1% trifluoroacetic acid) and applied to a matrix-assisted laser desorption/ionization (MALDI) targed plate. Pepetide mass was analyzed using AXIMA CFR MALDI time-of-flight (MALDI-TOF) mass spectrometer (Shimadzu, Kyoto, Japan). The spectra were obtained in the positive-ion reflector mode with delayed extraction. External calibration was performed using des-Arg-bradykinin $[M + H]^+ = 904.5$ (monoisotopic), and adrenocorticotropic hormone (ACTH) $[M + H]^+ = 2465.7$ (monoisotopic). Peptide mass fingerprinting [phenylmethylsulfonyl fluoride (PMSF)] database search was performed by sending the list of observed masses to MASCOT search engine *http://www.matrixscience.com/*

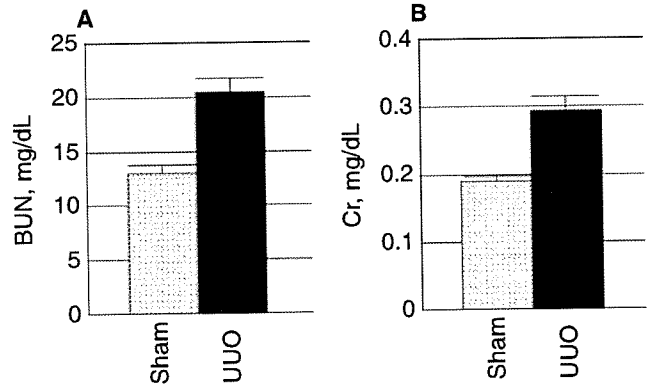

Fig. 1. Biochemical parameters 1 week after operations. Blood urea nitrogen (BUN) levels (*A*) were significantly increased in the unilateral ureteral obstruction (UUO)-treated rats (■) (20.5 ± 1.25 mg/dL) above those in recipients of sham-operation (□) (12.9 ± 0.83 mg/dL) ($P < 0.01$). Similarly, serum creatinine (Cr) (*B*) of UUO group (■) (0.29 ± 0.02 mg/dL) was significantly elevated compared with that of the sham-operated group (□) (0.19 ± 0.01 mg/dL) ($P < 0.01$).

Statistical analysis

All values are expressed as means ± SEM. Statistical significance between groups was determined by the unpaired *t* test. *P* values less than 0.05 were considered statistically significant.

RESULTS

Renal damage was induced by UUO

One week after surgery to place ureteral obstructions in the left kidneys of rats ($N = 6$), serum levels of BUN and creatinine were measured to confirm whether the UUO procedure caused subsequent renal failure. Serum BUN levels in these animals were significantly greater than those in sham-operated group ($N = 6$) (20.5 ± 1.25 mg/dL vs. 12.9 ± 0.83 mg/dL) ($P < 0.001$) (Fig. 1). Similarly, serum creatinine levels in the UUO group exceeded those in the sham-operated group (0.29 ± 0.02 mg/dL vs. 0.19 ± 0.01 mg/dL) ($P < 0.01$) (Fig. 1).

Histologically, renal tissues of sham-operated rats appeared normal under the light microscope (Fig. 2A and B). One week after surgery, glomeruli in the right (contralateral), unobstructed kidneys of UUO group were almost normal (Fig. 2C), whereas glomeruli of the obstructed left kidneys were shrunken, with cuboidal

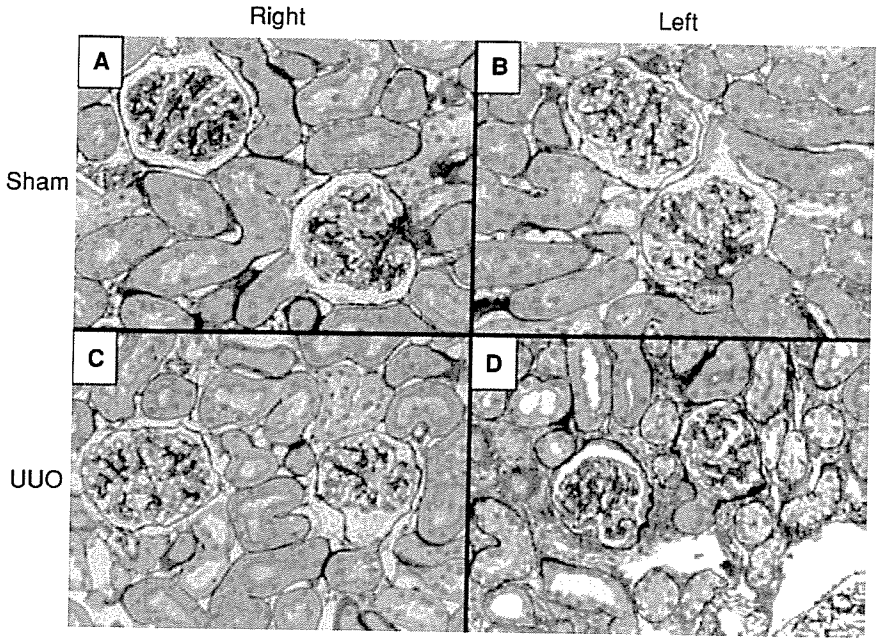

Fig. 2. Light microscopic findings 1 week after the operations. Under the light microscope, periodic acid-methenamine-silver (PAM) staining of kidney sections 1 week after unilateral ureteral obstruction (UUO) or sham-operation (Sham) showed that glomeruli and interstitium from right kidneys (*A*) and left kidneys (*B*) of sham-operated rats were normal. Similarly, unobstructed right kidneys from rats whose left kidneys received UUO had normal glomeruli (*C*). However, in UUO-treated left kidneys (*D*), not only interstitial expansion was observed, but also thickened Bowman's capsules and cuboidal changes of parietal epithelial cells (original magnifications ×200).

parietal epithelium and fibrosis around Bowman's capsule (Fig. 2D). The expansion of interstitial area was also observed in the obstructed kidneys. These results present a clear picture of surgically induced obstructive nephropathy.

PAD type II mRNA was detected in kidney samples

The expression of PAD mRNAs was assessed by RT-PCR using individual primers for rat PAD type I, type II, type III, and type IV. However, no mRNA of PAD type I or type III was detected in samples from obstructed, contralateral or healthy control kidneys (Fig. 3B and C, lanes 1 to 4). Because mRNAs of the same samples from experimentally manipulated kidneys were amplified by primers of GAPDH (Fig. 3A, upper bands of lanes 1 to 5), and positive controls from epidermis expressing all PADs (Fig. 3A to D, lane 5) were also amplified by primers of PAD type I and type III, we verified that these samples were suitable for detection of the mRNA of interest. Like PAD types I and III, PAD type IV mRNA was seldom expressed in obstructed, contralateral or healthy control kidneys (Fig. 3D, lanes 1 to 4). Again, the suitability of extracted mRNA and primers of PAD type IV (Fig. 3A to D, lane 5) for these assays was confirmed. In contrast to the foregoing results in which PAD type I, III, and IV were not expressed, PAD type II mRNA was detected in all samples from the cortexes of normal as well as damaged kidneys (Fig. 3A, lanes 1 to 4). Relative PAD type II mRNA expression (PAD type II/GAPDH) is the highest in the left kidney with the obstruction (Fig. 3E).

Amounts of PAD type II protein increased in obstructed kidneys

Next, expression of PAD type II was examined by Western blot analysis. As shown in Figure 4, PAD type II protein was only minimally detectable in kidneys of sham-operated rats and the right contralateral kidneys of the UUO group (Fig. 4A, sham left and UUO right). However, PAD type II protein of approximately 70 kD was observed in the left kidneys of the UUO group (Fig. 4A, UUO left). The specificity of rabbit anti-PAD type II antibody used to identify the protein was reconfirmed when no bands were detectable with rabbit serum used as a first antibody instead of anti-PAD type II antibody (Fig. 4C). Additionally, the extracted proteins were stained by CBB (Fig. 4B and D). When protein bands were quantified by densitometry, PAD type II protein was significantly increased in obstructed kidneys (Fig. 4E).

Obstructed kidneys developed large increases in citrullinated proteins

The expression of the PAD type II does not always catalyze citrullination, because this reaction requires Ca^{2+}. However, Western blot analysis using specific antibody against modified citrulline residues successfully yielded bands of approximately 70 kD, 60 kD, and 40 kD, denoting the presence of citrullinated proteins on chemically treated membranes only in obstructed kidneys of the UUO group (Fig. 5A, UUO left). To the contrary, in the kidneys of sham-operated rats and contralateral kidneys of the UUO animals, no such bands appeared (Fig. 5A, sham left and UUO right). Because this antibody does not react with unmodified citrulline, we can certify the

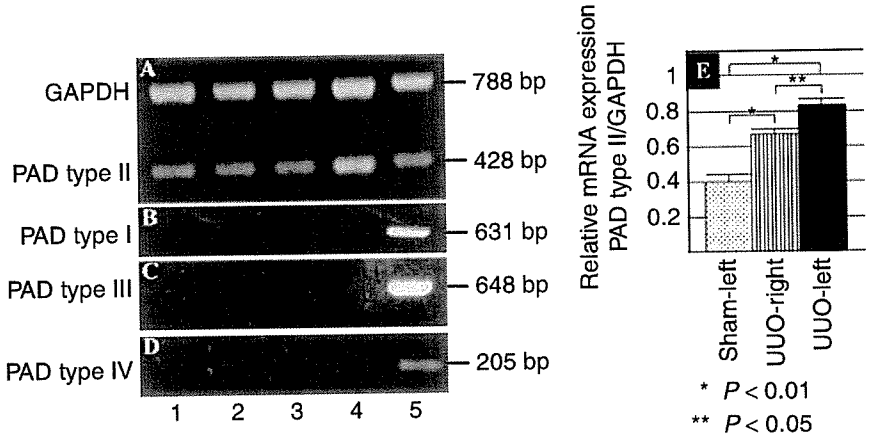

Fig. 3. Expression of glyceraldehyde-3-phosphate dehydrogenase (GAPDH) (*A*), peptidylarginine deiminases (PAD) type I (*B*), type II (A), type III (*C*), and type IV (*D*) transcripts in rat kidneys. Total RNA was isolated from the cortexes of rat kidneys, and the same templates from experimented kidneys were amplified by reverse transcription-polymerase chain reaction (RT-PCR) using each primer. Lane 1, right kidney with sham-operation; lane 2, left kidney with sham-operation; lane 3, right (contralateral) kidney with unilateral ureteral obstruction (UUO) treatment; lane 4, left kidney (obstructed) kidney with UUO; lane 5, positive control from rat epidermis. Expected sizes of amplified sequences based on primer design were 631 bp for PAD type I, 428 bp for PAD type II, 648 bp for PAD type III, 205 bp for PAD type III, and 788 bp for GAPDH. All PADs transcripts were observed in epidermal samples and all samples were amplified by primers of GAPDH. PAD type II mRNA was detected only in kidney tissue, regardless of obstruction or lack thereof (A). PAD type I (B), III (C), and IV (D) mRNA were merely detected in samples from obstructed, contralateral, or healthy control kidneys. Relative amount of PAD type II mRNA expression (PAD type II/GAPDH) is the highest in left kidneys with the obstruction (*E*). Values are mean ± SEM.

specificity of this antibody by staining membranes without chemical treatment. As shown in Fig. 5C, no bands emerged on the membrane without chemical modification. The extracted proteins were stained by CBB staining (Fig. 5B and D).

PAD type II protein was preferentially expressed in parietal epithelial cells of kidneys damaged by obstruction but not in normal kidneys

By immunohistochemical analysis, PAD type II expression was barely noticeable along the parietal epithelia of normal rat kidneys (Fig. 6A and B, Sham) or in unobstructed kidneys (Fig. 6C, UUO right). On the other hand, PAD type II expression was marked in parietal epithelia of tissue undergoing obstructive nephropathy 1 week after the UUO operation (Fig. 6D, UUO left). No PAD type II expression was observed except on glomerular parietal epithelial cells. As shown in Table 1, 1 week after UUO, intensity of PAD type II expression in Bowman's capsules and percentages of PAD type II–positive glomeruli were significantly increased in left kidneys of UUO group (UUO left 1 week) compared with those of contralateral kidneys (UUO right 1 week) or sham-operated kidneys (Sham left).

Citrullinated protein is preferentially present along Bowman's capsule

When we proceeded with staining to identify citrullinated proteins in situ, almost no citrullinated proteins appeared in kidneys of sham-operated rats (Fig.7A and B). Sometimes, a few citrullinated proteins lay along Bowman's capsule in a very small number of glomeruli of the sham-operated group. Similarly, citrullinated proteins were scarce in right contralateral kidneys of the UUO group (Fig. 7C). To the contrary, citrullinated proteins were visible along Bowman's capsule of the obstructed left kidneys (Fig. 7D). When we stained rat kidney tissues without chemical treatment by the modification medium, no positive staining was seen at all (Fig. 7E to H). Therefore, the specificity of the antibody used was reconfirmed histochemically, and this procedure showed that PAD type II and citrullinated proteins both lodged preferentially along Bowman's capsules of damaged kidneys by UUO. One week after UUO, staining intensity for citrullinated proteins in Bowman's capsules and percentages of positive glomeruli were markedly higher in the left obstructed kidneys of UUO group than right unobstructed kidneys or sham-operated kidneys (Table 1).

Citrullination decreased by the release of ureteral obstruction

To investigate whether citrullination reflects kidney damages by UUO, ureter-bladder anastomosis was made 1 week after the UUO operation. Glomeruli of the left kidneys with UUO for 5 weeks had cuboidal parietal epithelium and periglomerular fibrosis around Bowman's capsule (Fig. 8A). Four weeks after the release of ureteral obstruction, glomeruli returned to normal, and its parietal epithelium became flat (Fig. 8B). This light

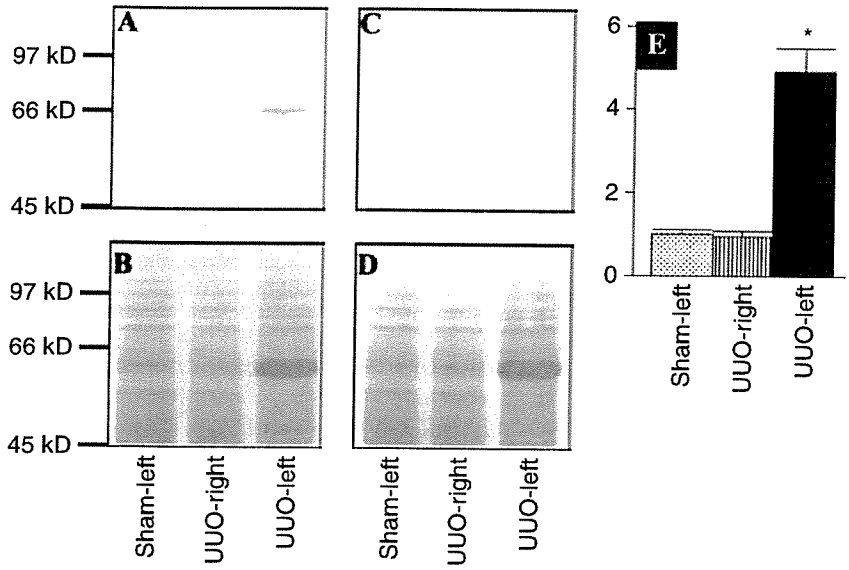

Fig. 4. Western blot for peptidylarginine deiminases (PAD) type II. A total 30 μg of isolated proteins from kidney cortexes was transferred to polyvinylidine difluoride (PVDF) membranes. Bands positive for PAD type II scarcely appeared in sham-operated (Sham-left) or unobstructed kidneys of unilateral ureteral obstruction (UUO) group (UUO-right). In contrast, a clear band at approximately 70 kD was observed in left kidneys 1 week after UUO (UUO-left) (*A*). Thereafter, the membrane was stained by Coomassie brilliant blue (CBB) (*B*). Although bands at approximately 60 kD and 80 kD were more intense in left kidneys of the UUO group than others, intensities of other bands were similar. When the membranes stained by rabbit serum as a first antibody instead of anti PAD type II antibody, no bands were visible (*C*). Therefore, the band in (A) is specific. That membrane was stained by CBB (*D*). When protein bands were quantified by densitometry, PAD type II amount was significantly increased in left obstructed kidneys (UUO-left) compared with that in sham-operated kidneys (Sham-left) or contra-lateral kidneys (UUO-right) (Fig 4E). $^*P < 0.01$ versus sham-operated kidneys and right contra-lateral kidneys with UUO. Values are mean ± SEM.

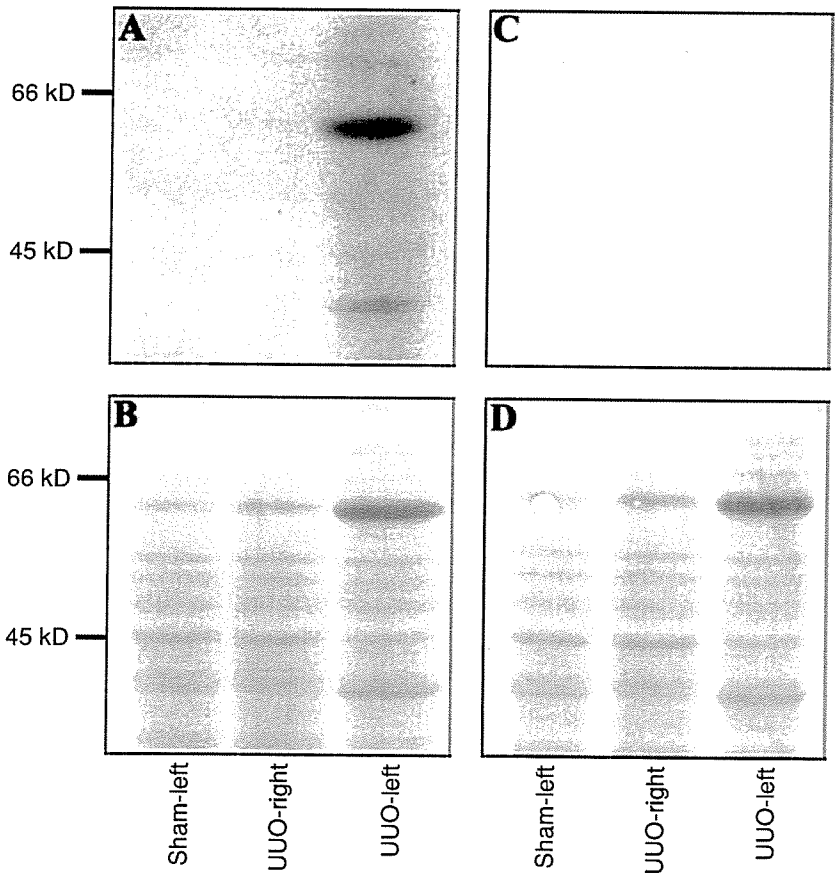

Fig. 5. Western blot for detection of citrullinated proteins. A total 30 μg of proteins isolated from kidney cortex was transferred to polyvinylidine difluroride (PVDF) membranes. For detection, monoclonal antibody was added to react chemically with modified citrulline. One membrane was treated with the modification medium before the reaction with anti-modified citrulline antibody, and then citrullinated proteins were stained as described in the Methods section (*A*), followed by Coomassie brilliant blue (CBB) staining (*B*). Citrullinated proteins were detected only in obstructed kidneys (UUO-left) (A). Another membrane was stained by same first antibody and second antibody without chemical modification as a control (*C*), followed by CBB staining (*D*). No bands of citrullinated proteins were observed in the membrane without chemical modification (C), which indicated specific reaction of first antibody to chemically modified citrulline.

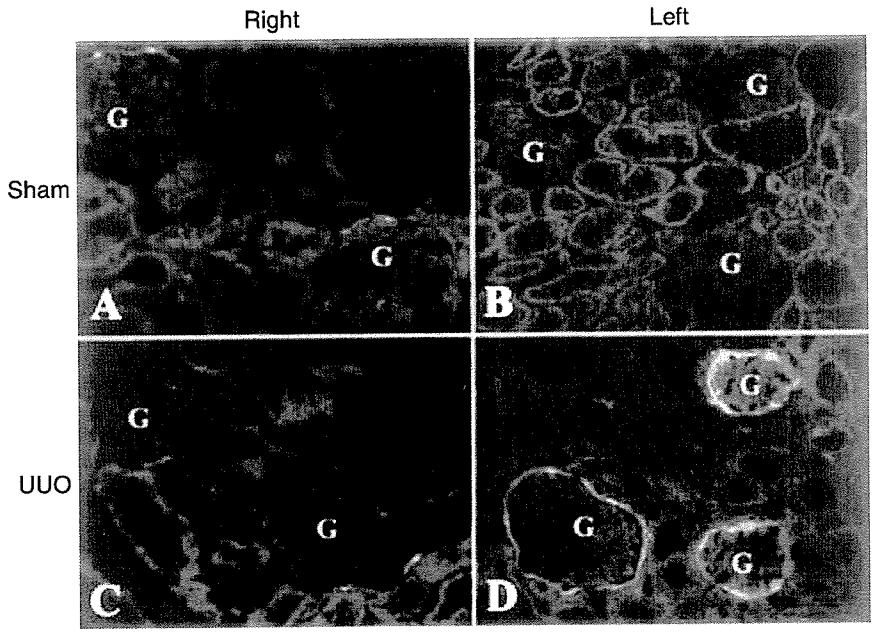

Fig. 6. Peptidylarginine deiminases (PAD) type II expression on abnormal Bowman's capsules. Kidney tissues were stained by rabbit antirat PAD type II antiserum. (*A*) Right kidney of sham-operated group. (*B*) Left kidney of sham-operated group. (*C*) Right kidney of unilateral ureteral obstruction (UUO) group. (*D*) Left kidney with ureteral obstruction of UUO group. In both sides of kidneys in sham-operated group, PAD type II expression was miniscule (A and B). In contralateral, unobstructed kidney (right), the expression was also scarce (C). On the other hand, in left kidneys staining for PAD type II was positive and located preferentially in parietal epithelial cells of Bowman's capsules (D). G is a glomerulus (original magnifications ×200).

Table 1. Summary of histologic examinations (the semiquantitative values of staining intensity and percentages of positive glomeruli for peptidylarginine deiminase (PAD) type II and citrullinated proteins

Group	PAD II		Citrullinated protein	
	Intensity	%	Intensity	%
Sham left ($N = 6$)	0.63 ± 0.14	36.9 ± 3.7	0.13 ± 0.04	9.2 ± 2.9
UUO right 1 week ($N = 6$)	0.76 ± 0.12	40.7 ± 4.5	0.08 ± 0.03	8.1 ± 2.7
UUO left 1 week ($N = 6$)	$3.64 \pm 0.13^{a,c}$	$100 \pm 0^{a,c}$	$1.71 \pm 0.06^{a,c}$	$92.1 \pm 1.8^{a,c}$
UUO left 5 week ($N = 4$)	$4.00 \pm 0.00^{a,c}$	$100 \pm 0^{a,c}$	$3.02 \pm 0.24^{a,c,d}$	$100 \pm 0^{a,c,d}$
Bypass left 5 week ($N = 4$)	$2.61 \pm 0.22^{a,c,d,e}$	$80.1 \pm 3.8^{a,b,c,d,e}$	$0.33 \pm 0.06^{b,c,d,e}$	$27.8 \pm 6.0^{b,c,d,e}$

UUO is unilateral ureteral obstruction; Bypass left 5 weeks, the data from rats receiving ureter-bladder bypass 1 week after UUO and then living for 4 weeks. The calculation methods of staining intensity and percentages were explained in the **Methods** section. Values are mean ± SEM. Statistical significance between groups was determined by the unpaired *t* test.

[a] $P < 0.01$ versus sham; [b] $P < 0.05$ versus sham; [c] $P < 0.01$ versus right contralateral kidneys of UUO group for 1 week (UUO right 1week); [d] $P < 0.01$ versus left obstructed kidneys after 1-week ligation (UUO left 1weed); [e] $P < 0.01$ versus left obstructed kidneys after 5 weeks of UUO (UUO left 5 weeks).

microscopic study showed that the lesions in Bowman's capsules with UUO were attenuated by the ureter-bladder anastomosis to release the ureteral obstruction. Five weeks after UUO operation, PAD type II expression was strongly observed in the whole parietal epithelial cells (Fig. 8C) (Table 1). This intense expression of PAD type II was significantly attenuated by the release of ureteral obstruction (Fig. 8D) (Table 1). Citrullinated proteins were also increased in Bowman's capsules of obstructed kidneys for 5 weeks (Fig. 8E) (Table 1). However, when we performed the operation for release of UUO 1 week after the ureteral ligation, the citrullinated proteins were diffusely decreased below those in kidneys with UUO for 5 weeks. Furthermore, PAD type II and citrullinated proteins were also significantly diminished in the left kidneys of the group that underwent the ureter-bladder bypass operation even compared with those in the left obstructed kidneys for 1 week, in which these proteins were already increased in Bowman's capsules (Table 1).

Actin filaments should be citrullinated in the kidney

Next, two-dimensional electrophoresis was performed to investigate what proteins were citrullinated in the kidney. We obtained two spots which were citrullinated (Fig. 9). Their molecular weights were both approximately 40 kD. The MALDI mass fingerprint spectrums of these spots at 40 kD (Fig. 10A) were analyzed by the MASCOT search engine. The results showed that citrullinated proteins at 40 kD were actins (Fig. 10B).

DISCUSSION

This report describes for the first time that PAD type II and citrullinated proteins are suitable markers for Bowman's capsules, since their expression occurs preferentially in Bowman's capsules of the renal glomeruli and increases markedly during the course of obstructive nephropathy.

For this study, we adapted a model of obstructive renal damage by unilaterally ligating the left ureter (UUO) in

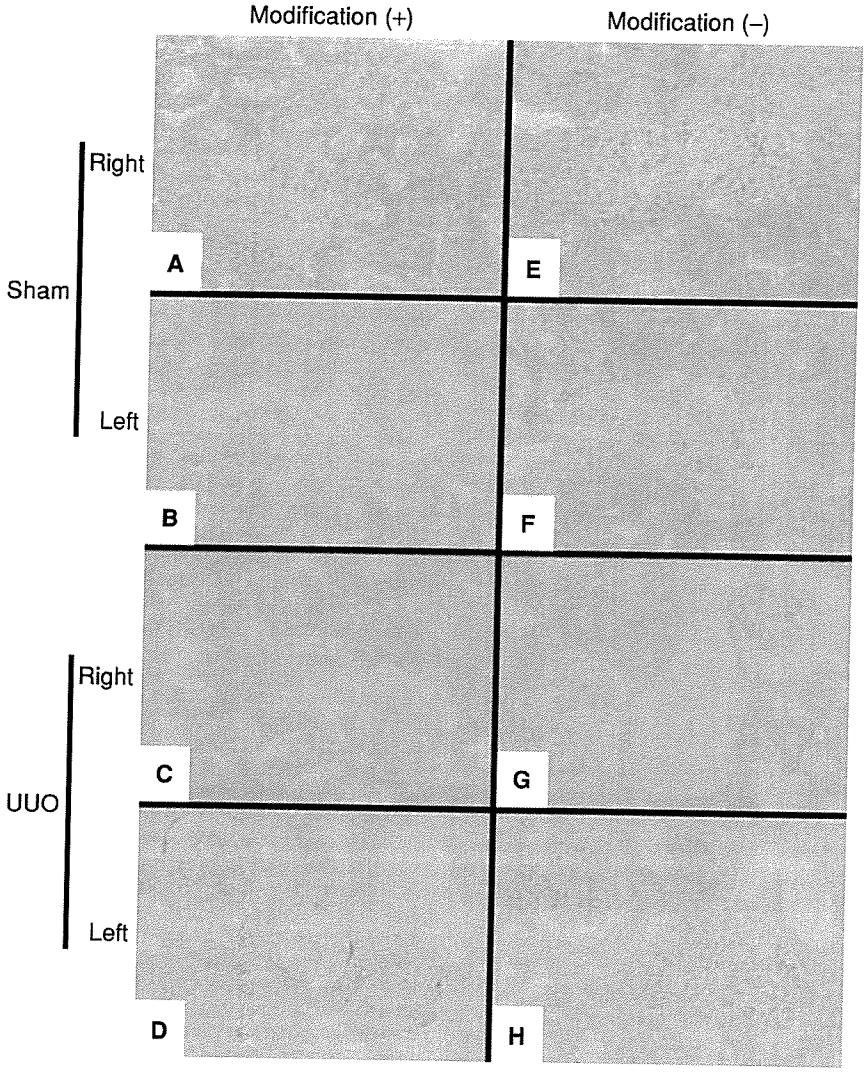

Fig. 7. Detection of citrullinated protein in situ. Citrullinated proteins were detected by modification of citrulline residues in tissues followed by staining with anti modified citrulline antibody. (*A* and *E*) Right kidney of sham-operated group. (*B* and *F*) Left kidney of sham-operated group. (*C* and *G*) Right unobstructed kidney of unilateral ureteral obstruction (UUO) group. (*D* and *H*) Left obstructed kidney of UUO group. When tissues were stained after chemical modification (A to D), both sides of sham-operated group and right kidney of UUO group did not show positive staining for citrullinated proteins (A to C). Only in the left obstructed kidney of the UUO group was protein citrullination was preferentially detected in Bowman's capsule, which appeared like rings (D). When tissues were not chemically modified (E to H), no positive staining followed (original magnifications ×200).

each of six rats and simultaneously performed sham operations as a control ($N = 6$). UUO increases fluid pressure in the urinary tract, thereby also increasing pressure in tubuli and Bowman's space. This model has been used often to study the mechanisms of renal fibrosis [16]. In the glomeruli, UUO makes parietal epithelial cells of Bowman's capsule receive tension as mechanical stress. In this study, UUO of the rat urinary tract caused renal failure within 1 week, as confirmed by increases of serum BUN and creatinine (Fig. 1). In addition, the obstructed kidneys had thickening of Bowman's capsules and cuboidal formation of the parietal epithelial cells (Fig. 2).

The results of RT-PCR to identify PADs indicated that neither PAD type I nor type III was expressed in any kidneys, whether normal, UUO operated, or sham operated (Fig. 3). Similarly, PAD type IV was rarely detected in any of these kidneys (Fig. 3), and even this limited expression of PAD type IV mRNA seemed to come from circulating leukocytes left after presurgical perfusion, because these cells do express PAD type IV [17]. A marked difference was the expression of PAD type II mRNA found in both right and left kidneys of the UUO group and the sham-operated group (Fig. 3). Therefore, we judged that renal cells express only type II of the four known PAD types. When we measured the densities of bands and calculated relative amounts of PAD type II mRNA/GAPDH mRNA, amounts in the rats' left obstructed kidneys were significantly higher than in any other samples of kidneys from sham-operated rats or right kidneys from the UUO group (Fig. 3E). This increase of PAD type II in obstructed kidneys was confirmed by Western blot of protein levels (Fig. 4). Sham-operated and unobstructed kidneys had only negligible levels of PAD type II, whereas the bands of PAD type II were readily detected at the expected molecular weight in all obstructed kidneys from the UUO group. Therefore, PAD type II is expressed by renal cells, and the amount increases after ureteral blockage (Fig. 4E). In addition, glomerular parietal epithelial cells of obstructed kidneys preferentially express PAD type II, but those of normal kidneys (Fig. 6). Because